COMBINED STEAM AND CO_2 REFORMING OF CH_4 OVER NICKEL CATALYSTS BASED ON Al_2O_3–MO (M= Mg, Ca, Ba)

Phuong P. H. [1], Loc L.C. [1, 2, *], Sang P. T. [1], Tri N. [2]

[1]*Oil & Gas Processing Department, Faculty of Chemical Engineering, HCMUT–VNUHCM*
268 Ly Thuong Kiet Street, Ward 14, District 10, Ho Chi Minh City, Vietnam

[2]*Institute of Chemical Technology, Vietnam*
1 Mac Dinh Chi Street, Ben Nghe Ward, District 1, Ho Chi Minh City, Vietnam

[*]Email: *camloc.luu@gmail.com*

Received: 30 December 2016; Accepted for publication: 2 March 2017

ABSTRACT

A series of 10 wt% Ni/Al_2O_3–MO (M = Mg, Ca, Ba) catalyst was prepared by impregnation method for applying in the combined steam and carbon dioxide reforming of methane (CSCRM). In this study, five supported nickel catalysts were impregnated on different supports. All of the supports have been obtained by co–precipitation method and also have been investigated. Several techniques, including N_2 physisorption measurements, X–ray powder diffraction (XRD), temperature–programmed reduction using H_2 (H_2–TPR), and transmission electron microscopy (TEM) were used to investigate catalysts' physicochemical properties. The results showed that MgO was the most suitable promoter comparing with CaO and BaO in CSCRM. The presence of MgO in Ni/Al_2O_3 changed catalysts' characteristics leading to an increase in the catalytic activity and stability with time on stream (TOS). It was found that the suitable catalyst was Ni–based on Al_2O_3–MgO of mass ratio 2:1 which showed a high metal dispersion as well as dominated spinel structure. The CH_4 and CO_2 conversion at 800 °C reached 99.8 % and 51.7 %, respectively. Catalytic stability of this catalyst with TOS at 800 °C could reach to more than 20 hours until it started decreasing.

Keywords: CH_4 bi–reforming, combined steam and CO_2, Ni–based catalysts, Al_2O_3–MgO supports.

1. INTRODUCTION

The conversion of hydrocarbons to hydrogen and syngas plays an important role in the 21st century ranging from gas to liquid to hydrogen plants. Natural gas contains between 70 and 98% of methane, with higher hydrocarbon, while diluents (N_2, CO_2) can account for a maximum of 15%, depending on the location from where it is produced [1]. The Fischer–Tropsch (F–T) synthesis is understandably regarded as the key technological component of schemes for converting syngas to transportation fuels and other liquid products. CSDRM appears as a promising way to make use of CO_2 rich natural gas and achieve the syngas with ratio H_2/CO around of 2, which is suitable for F–T reaction. Ni is by far the most favorable and common

metal used for industrial reforming processes due to high efficiency compared with other metal such as Pt, Pd, etc... for a long time ago. Beside the active metals of the catalyst, the most common support used in industry is Al_2O_3. Other supports like MgO, TiO_2, SiO_2, and La_2O_3 were also used [2]. It is believed that the significant effect of support may be due to a direct activation of CH_4 or CO_2 by metal oxides and the difference of particle size of the metal [3]. Ni/MgO–Al_2O_3 catalyst with high resistance to coke formation had been successfully developed for CSCRM by using hydrotalcite–like material as a precursor [4]. Especially, the catalyst promoted with 6 wt%. Ce showed the highest effect as well as outstanding coke resistance due to improved dispersion of Ni as well as oxygen loaded capability of CeO_2 [5]. However, a detailed study about the role of different alkaline earth metals in CSCRM is not fully reported so far. In this study, the influence of various alkaline earth metal with different loading content on catalytic performance CSCRM as well as their physicochemical properties were investigated.

2. EXPERIMENT AND PREPARATION

2.1. Catalyst preparation

A solution of $M(NO_3)_m.nH_2O$ ($Mg(NO_3)_2.6H_2O$,$Ca(NO_3)_2.4H_2O$ or $Ba(NO_3)_2$ – Xilong, ≥ 99 %) and $Al(NO_3)_3.9H_2O$ (Xilong, ≥ 99 %) followed by desired MO:Al_2O_3 mass ratio was obtained. After that, the MO–Al_2O_3 support was prepared by simultaneous drip at 60 °C between the above solution and 5% NH_3 solution. The obtained suspension was then stirred regularly in 30 minutes before overnight aging and evaporation at 80–90 °C. The raw solid was then dried at 110 °C in 12 hours before calcination at 800 °C in 3 hours to obtain the final supports. An amount of $Ni(NO_3)_2.6H_2O$ (Xilong, > 99 %) was calculated based on a desirable mass proportion of the metal active sites on catalyst. It was then dissolved in distilled water. A suitable quantity of support was dispersed into distilled water in another beaker. Subsequently, nickel was impregnated on the supports at 60 ÷ 70 °C by pouring the former solution into latter beaker and the magnetic stir was used to disperse the solid equally.

When the raw solid was achieved, it was continuously dried at 110 °C in 12 hours before calcination at 800 °C in 3 hours.

The catalysts are symbolized as follows: percentage of Ni not shown in all catalysts being 10 wt%, element symbols immediately followed by the ratio indicating the weight ratio of MgO:Al_2O_3 in the catalyst. For example: NiO/(MgO–Al_2O_3) (1:1) is the catalyst containing 10 wt.% Ni and weight ratio of MgO:Al_2O_3 of 1:1.

2.2. Characterization

The crystaline structure of prepared catalysts were investigated by X–ray diffraction using Bruker D2 Phaser powder diffractometer with CuKα radiation (λ = 0.15406 nm) varying 2θ in the range of 10–80°. The analysis was recorded at the Center for Innovative Materials and Architectures (INOMAR–VNUHCM). The surface area of these catalysts were measured by BET (Nova Station B, Quantachrome NovaWin Instrument) through the nitrogen adsorption at –196 °C at INOMAR–VNUHCM. Temperature programmed reduction (TPR, Micromeritics, Autochem 2910) was carried out to identify the reduction temperature and H_2 consumption of catalysts at Institute of Chemical Technology (ICT–VAST). Metal particle size dispersed on support is characterised by Transmission electron microscopy (TEM) using JEOL JEM 1400 instrument at National Key Lab for Polymer and Composite Materials.

2.3. Catalytic Testing

Activity of the catalysts was determined in a quartz reactor under atmospheric pressure at 800 °C after reduction in 40% H_2/Ar within 3 hours at 800 °C. The weight of catalyst sample was 1 gram mixed with 2 grams of quartz. The feed ratio of $H_2O/CO_2/CH_4$ was fixed at 2.4/1.2/3 and space velocity was 15530 cm^3 gas fed/g_{cat}.h. The reaction mixture was analyzed on the Automatic Gas Chromatograph (AGC 600) with a TCD detector and MS – 13X column (3 m length; 30/60) connected with Porapack N column (3 m length; 50/80). The calculation equation of CH_4 conversion, CO_2 conversion, H_2 yield, CO yield, H_2/CO molar ratio was followed:

$$CH_4 \text{ conversion } (\%) = \frac{[CH_4]_{in} - [CH_4]_{out}}{[CH_4]_{in}} \text{ x } 100\% \quad (1)$$

$$CO_2 \text{ conversion } (\%) = \frac{[CO_2]_{in} - [CO_2]_{out}}{[CO_2]_{in}} \text{ x } 100\% \quad (2)$$

$$H_2 \text{ yield } (\%) = \frac{[H_2]_{out}}{2[CH_4]_{in} + [H_2]_{in}} \text{ x } 100\% \quad (3)$$

$$CO \text{ yield } (\%) = \frac{[CO]_{out}}{[CH_4]_{in} + [CO_2]_{in}} \text{ x } 100\% \quad (4)$$

$$H_2 / CO = \frac{[H_2]_{out}}{[CO]_{out}} \quad (5)$$

3. RESULTS AND DISCUSSION

3.1. Catalyst Characterization

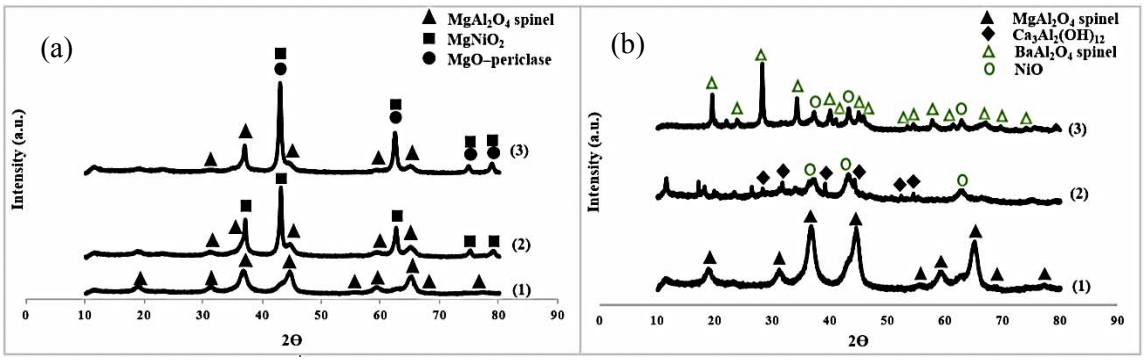

Figure 1. XRD pattern of (a) Ni/MgO–Al_2O_3 catalysts with different MgO loading content: (1) NiO/(MgO–Al_2O_3) (1:2), (2) NiO/(MgO–Al_2O_3)(1:1), (3) NiO/(MgO–Al_2O_3) (2:1) and (b) Ni/MO–Al_2O_3 catalysts with different alkaline earth metal: (1) NiO/(MgO–Al_2O_3) (1:2), (2) NiO/(CaO–Al_2O_3) (1:2), (3) NiO/(BaO–Al_2O_3) (1:2).

Figure 1a illustrates XRD results of three unreduced NiO/(MgO–Al_2O_3) catalysts which were prepared by co–precipitation methods and impregnation methods subsequently. As is highlighted on the chart, all of the catalysts demonstrate an appearance of peaks which indicated an existence of spinel crystallite phase $MgAl_2O_4$. These results release an interpretation that the absence of any NiO peak in the XRD spectrum confirms a high dispersion of NiO phase on the support [6]. However, in NiO/(MgO–Al_2O_3) (1:1) catalyst, the peaks representing the $MgNiO_2$

phase at 2θ = 38°, 43°, 62.7°, 75° and 79° are detected. This phase reveals the formation of solid solution between NiO and MgO. On the other hand, NiO/(MgO–Al_2O_3) (2:1) catalyst shows the presence of MgO–periclase at 2θ = 43°, 62°, 74.7° and 78.5°. It could be concluded that independent peaks of the NiO–MgO solid solution and MgO–periclase phases overlapped in this catalyst. NiO and MgO are principally the same structure and the difference in bond distances [7]. In addition, it is obvious that the periclase phase becomes dominant by increasing the amount of MgO placed in the catalyst [8].

By the way, it is noticeable in Figure 1b that, in NiO/(CaO–Al_2O_3) (1:2) catalyst, NiO phase (2θ = 37.2°, 43.2°, 62.8°) dominates compared with others. In addition, the peaks of $Ca_3Al_2(OH)_{12}$ phase at 2θ = 18°, 28°, 34° and 44° are also detected. It is the silicon free member of the garnet family of minerals, having a cubic structure in which Al is in an octahedral environment and Ca is eight coordinate in a square anti–prismatic arrangement [9].

On the other hand, as seen in Figure 1b, NiO/(BaO–Al_2O_3) (1:2) catalyst shows the existence of spinel $BaAl_2O_4$ phase (2θ = 19.5°, 22°, 28.2°, 34.2°, 40°, 38°, 45°, 46°, 53.5°, 54.5°, 57.9°, 58.5°). Furthermore, the presence of NiO phases in this catalyst shows less dispersion of NiO phases on the support surface. Moreover, no peaks of spinel $NiAl_2O_4$ have been observed for three catalysts. As reported, Ba incorporation in Ni/Al_2O_4 catalysts inhibits the diffusion of Ni into the alumina structure to form $NiAl_2O_4$ [10].

The results presented in Table 1 indicate that NiO/(MgO–Al_2O_3) (1:2) catalyst has by far the highest surface area with 74.66 m^2/g, being nearly half 150 m^2/g which is the S_{BET} value of γ–Al_2O_3 [11]. This might because the spinel phase increases thermal and mechanical stability of catalyst leading to a decrease in the surface area. Moreover, loading of MgO on the catalyst leads to a partial blockage of the γ–Al_2O_3 pores by MgO clusters and/or a partial collapse of the mesoporous structure. Thus, the surface area decreases when bigger amount of MgO was added, from 74.66 m^2/g in NiO/(MgO–Al_2O_3) (1:2) to 23.77 m^2/g in NiO/(MgO–Al_2O_3) (2:1).

Table 1. Structural properties of catalysts.

Catalyst	S_{BET} (m^2/g)[a]	$MgAl_2O_4$ crystallite diameter (nm)[b]	NiO crystallite diameter (nm)[b]
NiO/(MgO–Al_2O_3) (1:1)	–	2.869	–
NiO/(MgO–Al_2O_3) (2:1)	23.77	2.876	–
NiO/(MgO–Al_2O_3) (1:2)	74.66	2.857	–
NiO/(CaO–Al_2O_3) (1:2)	16.20	–	2.46
NiO/(BaO–Al_2O_3) (1:2)	–	–	2.41
[a] Obtained from N_2 adsorption at –196 °C [b] Estimated from XRD by using Debye–Scherrer equation [4]			

It is clear that the catalyst modified by CaO showed the lowest surface area. As aforementioned in XRD results, no spinel phase $CaAl_2O_4$ but either NiO crystallite phase or $Ca_3Al_2(OH)_{12}$ was observed. In addition, as in the table 1, an increase of NiO diameter on the catalyst modified by BaO and CaO respectively displays the fact that these alkaline earth metals show less dispersion and high sintering of NiO during calcination stage comparing with the one promoted by MgO.

Figure 2 shows the TEM result of the NiO/(MgO–Al_2O_3) (1:2) catalyst before reduction. As can be seen in the images, the catalyst which was prepared by co–precipitation method with low MgO content loaded displays the result that less than 5 nm of the support crystallite solids were observed. Moreover, it is clear that in the first picture, the spinel phases are desultorily

distributed with a small size and no agglomeration to form the bulk crystallite solid are observed.

The TEM result of NiO/(MgO–Al_2O_3) (1:2) and catalyst modified by CaO reveals different trends of the metal active sites. It is in accordance with the XRD results that no spinel phase of $CaAl_2O_4$ was identified except of an appearance of $Ca_3Al_2(OH)_{12}$ phase. Interestingly, the sintering of NiO phase crystallite solids was observed in this catalyst with a bulk amount of NiO particles. As can be seen in Figure 2a and 2c, the sintering of small nickel particles and the supports into the bulk occurred after 50 hours of reaction.

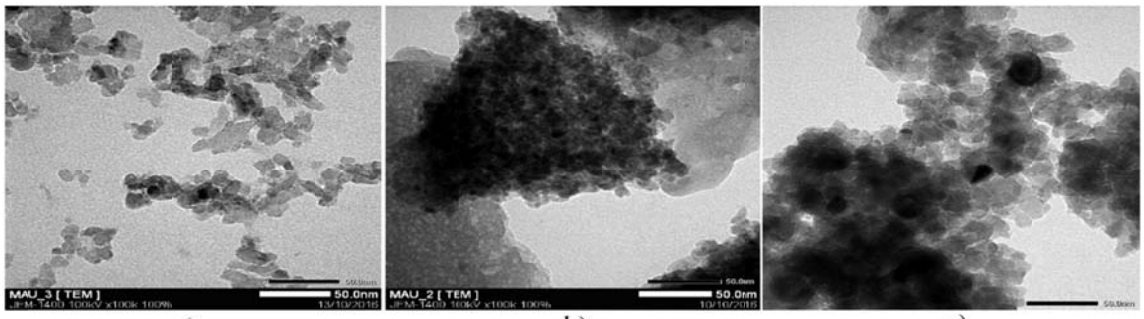

Figure 2. TEM images of catalysts; (a) NiO/(MgO–Al_2O_3) (1:2); (b) NiO/(CaO–Al_2O_3), and (c) used Ni/(MgO–Al_2O_3) (1:2).

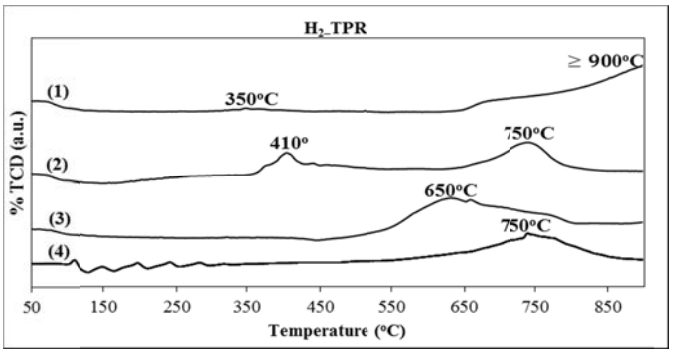

Figure 3. TPR patterns of catalysts: (1) NiO/(MgO:Al_2O_3) (2:1), (2) NiO/(BaO:Al_2O_3) (1:2), (3) NiO/(CaO:Al_2O_3) (1:2), (4) NiO/(MgO:Al_2O_3) (1:2).

As can be seen in the Figure 3, the reduction peaks of Ni^{2+} to form Ni^0 on the catalysts appear at two range of temperatures. The low temperature peak results from reduction of Ni^{2+} in the NiO phase while the high temperature peak most likely corresponds to Ni^{2+} in the mixed metal oxide phase ($Mg_xNi_{1-x}O$) [12]. The first peak of NiO/(BaO–Al_2O_3) (1:2) catalyst is identified as a reduction of NiO free particles which has weak interaction with the support. Interestingly, the second peak which appears at the temperature of around 750 °C displays the strong interaction of NiO with the support, the same with the result of the catalyst modified by MgO.

The catalyst modified by CaO shows the TPR result that there is only peak at 650 °C obtained, accounting for weaker support metal interaction compared with the two modified by MgO and BaO. It comes as no surprise that Mg is the most compatible alkaline earth metal used to modify Ni–based catalyst supported by Al_2O_3 for CSCRM. As the MgO/Al_2O_3 mass ratio

increases, TPR peaks the first at 350 °C and the second at higher temperature, above 900 °C, resulted from formation of NiO–MgO solid solution. As studied before, a major influencing factor to control the reduction of NiO in the solid solution is the isolation effect, because NiO is isolated by MgO, thus, the isolation effect inhibits the formation of the metal–metal bond during the reduction leading to prevent Ni aggregation [13]. In overall, the NiO/(MgO–Al_2O_3) (1:2) catalyst is expected to have better catalytic performance due to improved dispersion of Ni and stronger metal support interaction.

3.2. Catalytic Test

Table 2. Catalytic performance of five prepared catalysts.

T (°C)	X_{CH_4}(%)	X_{CO_2}(%)	Product Yield		H_2/CO
			Y_{H_2}(%)	Y_{CO} (%)	
NiO/(MgO–Al_2O_3) (1:2)					
800	99.87	66.66	62.47	62.54	2.00
NiO/(CaO–Al_2O_3) (1:2)					
800	99.46	58.16	65.88	60.64	2.17
NiO/(BaO–Al_2O_3) (1:2)					
800	99.57	77.95	65.76	75.69	1.64
NiO/(MgO–Al_2O_3) (1:1)					
800	99.85	65.54	63.19	62.88	2.15
NiO/(MgO–Al_2O_3) (2:1)					
800	99.30	60.79	65.27	57.49	2.27

The conversion of CH_4 (X_{CH_4}), conversion of CO_2 (X_{CO_2}), H_2 selectivity (Y_{H_2}), CO selectivity (Y_{CO}) and H_2/CO molar ratio in CSCRM at 800 °C on all five modified catalysts are clearly showed in Table 2. CH_4 conversion in the process carried on all catalysts nearly reaches to 100 %. As can be seen, among three catalysts promoted by MgO, the NiO/(MgO–Al_2O_3) catalyst (1:2) exhibits the highest CO_2 conversion. The biggest conversion of CO_2 at 800 °C is 66.66 % on NiO/(MgO–Al_2O_3) (1:2) catalyst while 65.54 % and over 60.79 % are obtained for the NiO/(MgO–Al_2O_3) (1:1) and NiO/(MgO–Al_2O_3) (2:1) catalyst, respectively. As studied before, it is most likely that the addition of MgO is favourable to CO_2 adsorption, resulting in the increase of CO_2 conversion. However, the catalytic activity results in Table 2 display the fact that increasing in MgO loaded in catalyst causes a decrease in CO_2 conversion. This result is confirmed in view of previous observations that the presence of high amount of basic promoters leads to a reduction of dry reforming reaction rate [14]. An addition of Mg increases the interaction between NiO and support, improves the reducibility and the electronic properties of catalysts. It might also increase the basicity of catalyst, which is beneficial for the absorption and activation of CO_2.

As seen in Table 2, it is clear that the catalyst modified by BaO shows the highest conversion of CO_2 reaching to nearly 78 %. It is in agreement with the conclusion that the NiBa catalyst allow a system with a low carbonation level, characterized by the formation of a highly stable Ba spinel [10]. In addition, the H_2 selectivity is approximately equal for all modified catalysts. However, the CO selectivity of the catalyst modified by BaO is by far the highest one leading to a lower H_2/CO ratio. It could be the result of the fact that NiBa catalyst is favourable

for dry reforming of CH_4 and reverse water–gas shift reaction.

In conclusion, NiO/(MgO–Al_2O_3) (1:2) catalyst is considered the best among all investigated from point of view of H_2/CO ratio, CH_4 conversion and CO_2 conversion.

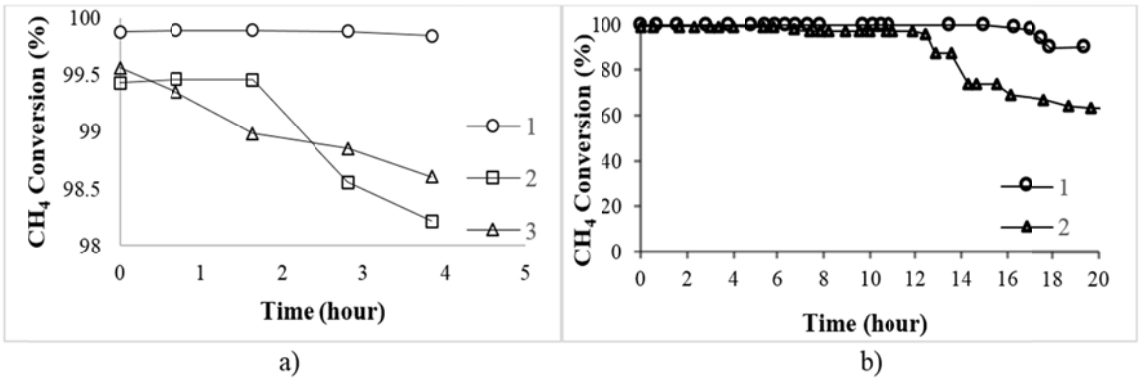

Figure 4. (a) Short time stability of (1) NiO/(MgO–Al_2O_3) (1:2), (2) NiO/(CaO–Al_2O_3) (1:2) and (3) NiO/(BaO–Al_2O_3) (1:2) reduced catalysts; (b) Long time stability of (1) NiO/(MgO–Al_2O_3) (1:2) and (2) NiO/(MgO–Al_2O_3) (2:1) reduced catalysts.

As highlighted in the Figure 4a, the catalyst modified by MgO shows the best performance throughout the short time test. The activity of this catalyst almost remains stable during 4 hours of reaction while the activity of the one modified by CaO is unchanged in 1.5 hours and then declines sharply. Another catalyst modified by BaO displays a gradual decrease during the time of performance test occurring. On the other hand, as can be seen in Figure 4b, the catalyst modified with lower MgO loaded amount exhibits a better performance than another. The activity of this one nearly remained stable in the first 15 hours and then slightly decreased to over 80 % after 21 hours from beginning. It comes as a surprise that higher amount of MgO loaded catalyst exhibited the activity that just leveled off in 13 hours and after that there was a significant decline in the next 8 hours. This rapid deactivation could be the result of a lower S_{BET} and presence of free NiO reduced at 350 °C as discussed in TPR pattern.

4. CONCLUSIONS

All the catalysts showed high activity towards combined reforming of methane. However, the catalyst modified by MgO with the 1:2 mass ratio with Al_2O_3 shows the most suitable performance for both CO_2 conversion and H_2/CO molar ratio. The $MgAl_2O_4$ spinel has large surface area and thermal stability. As increasing amount of MgO loaded on the catalyst, MgO is formed leading blockage of reduction of NiO species, resulting in less available Ni sites after the reduction and decrease in the surface area. An addition of Mg increases the interaction between NiO and support and influenced the reducibility, hence, increase capability of absorption and activation of CO_2.

Acknowledgements. This research is funded by Vietnam National University Ho Chi Minh City (VNU–HCM) under grant number **C2016–20–08**.

REFERENCES

1. Ross J., Van Keulen A. N. J., Hegarty M. E. S., Seshan K. – The catalytic conversion of natural gas to useful products, Catalysis Today **30** (1) (1996) 193–199.
2. Guo J., Lou H., Zhao Ho., Chai D., Zheng X. – Dry reforming of methane over nickel catalysts supported on magnesium aluminate spinel, Applied Catalysis A: General **273** (1) (2004) 75–82.
3. Roh H. S., Potdar H. S., Jun K.W. – Carbon dioxide reforming of methane over Ni catalysts supported on Al_2O_3 modified with La_2O_3, MgO, and CaO, Catalysis surveys from Asia **12** (4) (2008) 239–252.
4. Koo K. Y., Roh H. S., Seo Y. T., Seo D. J., Yoon W. L., Park S. B. – A highly effective and stable nano–sized Ni/MgO–Al_2O_3 catalyst for gas to liquids (GTL) process, International Journal of Hydrogen Energy **33** (8) (2008) 2036–2043.
5. Koo K. Y., Roh H. S., Jung U. H., Yoon W. L. – CeO_2 promoted Ni/Al_2O_3 catalyst in combined steam and carbon dioxide reforming of methane for gas to liquid (GTL) process, Catalysis letters **130** (1–2) (2009) 217–221.
6. Arena F., Frusteri F., Parmaliana A., Plyasova L., Shmakov A. N. – Effect of calcination on the structure of Ni/MgO catalyst: An X–ray diffraction study, Journal of the Chemical Society, Faraday Transactions **92** (3) (1996) 469–471.
7. Yoshida T., Tanaka T., Yoshida H., Funabiki T., Yoshida S. – Study on the dispersion of nickel ions in the NiO–MgO system by X–ray absorption fine structure, The Journal of Physical Chemistry **100** (6) (1996) 2302–2309.
8. Koo K. Y., et al. – Combined H_2O and CO_2 reforming of CH_4 over nano–sized Ni/MgO–Al_2O_3 catalysts for synthesis gas production for gas to liquid (GTL): Effect of Mg/Al mixed ratio on coke formation, Catalysis Today **146** (1) (2009) 166–171.
9. Fogg A. M., Freij A. J., Oliveira A., Rohl A. L., Ogden M. I., Parkinson G. M. – Morphological control of $Ca_3Al_2(OH)_{12}$, Journal of crystal growth **234** (1) (2002) 255–262.
10. García–Diéguez M., Herrera M. C., Pieta I. S., Larrubia M. A., Alemany L. J. – NiBa catalysts for CO_2–reforming of methane, Catalysis Communications **11** (14) (2010) 1133–1136.
11. Loc L. C., Phuong P. H. – Comparison of Pt–Sn/γ–Al_2O_3, Pt–Pb/γ–Al_2O_3 and Pt/γ–Al_2O_3 catalysts in dehydrocyclization of n–heptane at atmospheric pressure, Asean Engineering Journal **3 (**2) (2014) 37–45.
12. Schulze K., Makowski W., Chyzy R., Dziembaj R., Geismar G. – Nickel doped hydrotalcites as catalyst precursors for the partial oxidation of light paraffins, Applied clay science **18** (1) (2001) 59–69.
13. Hu Y. H. – Solid–solution catalysts for CO_2 reforming of methane, Catalysis Today **148** (3) (2009) 206–211.
14. Trimm D. L. – The formation and removal of coke from nickel catalyst, Catalysis Reviews Science and Engineering **16** (1) (1977) 155–189.